AGU PUBLICATIONS

Geochemistry, Geophysics, Geosystems

RESEARCH ARTICLE
10.1002/2014GC005239

Key Points:
- We observe both trench parallel and plate motion parallel fast directions
- Fast splitting directions correlate well with the age of subducting lithosphere

Supporting Information:
- ReadMe
- Supplementary Figures S1–S6
- Supplementary Tables S1–S2

Correspondence to:
C. Lynner,
colton.lynner@yale.edu

Citation:
Lynner, C., and M. D. Long (2014), Sub-slab anisotropy beneath the Sumatra and circum-Pacific subduction zones from source-side shear wave splitting observations, *Geochem. Geophys. Geosyst.*, *15*, 2262–2281, doi:10.1002/2014GC005239.

Received 10 JAN 2014
Accepted 11 MAY 2014
Accepted article online 15 MAY 2014
Published online 5 JUN 2014

Sub-slab anisotropy beneath the Sumatra and circum-Pacific subduction zones from source-side shear wave splitting observations

Colton Lynner[1] and Maureen D. Long[1]

[1]Department of Geology and Geophysics, Yale University, New Haven, Connecticut, USA

Abstract Understanding the dynamics of subduction is critical to our overall understanding of plate tectonics and the solid Earth system. Observations of seismic anisotropy can yield constraints on deformation patterns in the mantle surrounding subducting slabs, providing a tool for studying subduction dynamics. While many observations of seismic anisotropy have been made in subduction systems, our understanding of the mantle beneath subducting slabs remains tenuous due to the difficulty of constraining anisotropy in the sub-slab region. Recently, the source-side shear wave splitting technique has been refined and applied to several subduction systems worldwide, making accurate and direct measurements of sub-slab anisotropy feasible and offering unprecedented spatial and depth coverage in the sub-slab mantle. Here we present source-side shear wave splitting measurements for the Central America, Alaska-Aleutians, Sumatra, Ryukyu, and Izu-Bonin-Japan-Kurile subduction systems. We find that measured fast splitting directions in these regions generally fall into two broad categories, aligning either with the strike of the trench or with the motion of the subducting slab relative to the overriding plate. Trench parallel fast splitting directions dominate beneath the Izu-Bonin, Japan, and southern Kurile slabs and part of the Sumatra system, while fast directions that parallel the motion of the downgoing plate dominate in the Ryukyu, Central America, northern Kurile, western Sumatra, and Alaska-Aleutian regions. We find that plate motion parallel fast splitting directions in the sub-slab mantle are more common than previously thought. We observe a correlation between fast direction and age of the subducting lithosphere; older lithosphere ($>$95 Ma) is associated with trench parallel splitting while younger lithosphere ($<$95 Ma) is associated with plate motion parallel fast splitting directions. Finally, we observe source-side splitting for deep earthquakes (transition zone depths) beneath Japan and Sumatra, suggesting the presence of anisotropy at midmantle depths beneath these regions.

1. Introduction

The dynamics of subduction systems represents an important area of study in solid Earth science (see recent overviews by *Zhao* [2001], *van Keken* [2003], *King* [2007], *Billen* [2008], and *Long* [2013]). Understanding the structure and dynamics of the mantle in regions of subduction is crucial to our understanding of the role of subduction in the dynamic Earth system. The dynamics of the sub-slab mantle has only recently begun to be studied in great detail. This push to understand the dynamics of the sub-slab mantle has been driven by increased interest in the origin of the commonly observed trench parallel fast shear wave splitting directions beneath subducting slabs [e.g., *Russo and Silver*, 1994; *Long and Silver*, 2008, 2009; *Faccenda et al.*, 2008; *Song and Kawakatsu*, 2012, 2013; *Faccenda and Capitanio*, 2013; *Lynner and Long*, 2013]. This observation is striking, as it contravenes the predictions of the simplest two-dimensional models of sub-slab flow and the simplest scenarios for olivine lattice preferred orientation (LPO). A major outstanding question is whether the sub-slab mantle remains strongly coupled to the subducting slab, resulting in an entrained mantle layer, or whether the slab and the surrounding mantle are sufficiently decoupled to allow for escape or 3-D return flow.

Shear wave splitting is regarded as the most direct observational constraint on patterns of mantle flow [e.g., *Silver*, 1996; *Savage*, 1999; *Long and Becker*, 2010], as typical olivine fabrics in the upper mantle (A, C, or E-type) are such that the fast splitting direction aligns with the direction of maximum extensional strain [*Karato et al.*, 2008, and references therein]. Since olivine is the dominant upper mantle mineral, measurements of shear wave splitting (or other indicators of anisotropy) [e.g., *Silver and Chan*, 1991] can provide

© 2014. American Geophysical Union. All Rights Reserved.

information about patterns of upper mantle flow. Studies of anisotropy beneath subducting slabs typically identify fast splitting directions that are generally parallel to the trench; this pattern has been identified in many subduction zones worldwide [e.g., *Russo and Silver*, 1994; *Long and Silver*, 2008, 2009, and references therein]. In most regions, however, sub-slab anisotropy has been inferred by measuring the splitting of teleseismic phases (usually SKS and SKKS) and carrying out a correction for anisotropy in the mantle wedge based on measurements from local *S* waves. This method is plagued by poor depth resolution, the potential for errors due to the oversimplification of wedge anisotropy, and geographical constraints on both source and receiver geometries.

Originally applied by *Vinnik and Kind* [1993] and subsequently used by other studies [*Russo and Silver*, 1994; *Müller et al*., 2008a; *Russo*, 2009; *Russo et al*., 2010; *Foley and Long*, 2011; *Di Leo et al*., 2012; *Lynner and Long*, 2013; *Eakin and Long*, 2013], the source-side shear wave splitting method uses earthquakes located in subducting slabs and seismic stations located at teleseismic distances to probe the anisotropy of the sub-slab mantle. This method allows for substantially better spatial and depth resolution of anisotropy beneath a slab. In addition to improved coverage, source-side shear wave splitting has the benefit of completely avoiding any anisotropic signal from the mantle wedge, removing a major potential source of error. A limitation of this method, however, is that anisotropy beneath the receivers must be carefully characterized and any splitting of direct S phases due to receiver-side anisotropy must be removed in order to correctly identify the sub-slab anisotropic signal.

Here we present detailed source-side shear wave splitting measurements for the Izu-Bonin, Ryukyu, Northern Honshu, Kurile, Alaska-Aleutians, Central America, and Sumatra subduction systems. The measurements presented here complement our recent work on the Tonga [*Foley and Long*, 2011], Caribbean, and Scotia [*Lynner and Long*, 2013] regions and have allowed us to construct a uniform database of sub-slab splitting parameters for many subduction zones worldwide. We have chosen to focus on circum-Pacific subduction zones (including Sumatra) in this study, although we did not carry out measurements for South America as it is inconveniently located with respect to seismic stations at the relevant epicentral distances. A primary finding from this study is that trench parallel fast splitting directions beneath slabs are far from ubiquitous. We observe predominantly trench parallel fast splitting directions beneath Northern Honshu, Izu-Bonin, and portions of the Kurile (southern) and Sumatra (beneath eastern Indonesia) subduction zones. Interestingly, however, Ryukyu, the Alaska-Aleutians, Central America, and portions of the Sumatra and Kurile subduction zones exhibit fast directions that are roughly parallel to the motion of the downgoing plate. We observe a striking correlation between the observed fast directions and the age of the subducting lithosphere, with older slabs associated with trench parallel splitting and younger slabs associated with plate motion parallel splitting. In a companion paper (C. Lynner and M. D. Long, Testing models of sub-slab anisotropy using a global compilation of source-side shear wave splitting data, submitted to *Journal of Geophysical Research*, 2014), we use the measurements presented here as well as previously published source-side splitting data sets [*Foley and Long*, 2011; *Lynner and Long*, 2013] to test existing conceptual models of sub-slab anisotropy and develop a new model based on the plate age-dependent sub-slab splitting behavior documented here.

2. Tectonic Settings

The tectonic settings of the subduction zones examined in this study (e.g., age of the downgoing plate, slab dip, plate kinematics, slab morphology) vary a great deal. This allows us to examine several different potential variables that may be controlling sub-slab splitting. Here we provide a brief description of each of the subduction zones we investigated (Figure 1). All references to downgoing plate motions and velocities come from the MORVEL plate model of *DeMets et al*. [2010] and are in the reference frame of the upper plate (that is, we use the motion of the downgoing plate relative to the overriding plate). This is a suitable reference frame for evaluating plate motion as many aspects of subduction are controlled by characteristics of the subducting plate in relation to the overriding plate [e.g., *Lallemand et al*., 2005; *Schellart*, 2007]. As discussed in section 4, however, our choice of reference frame does not greatly impact interpretations of sub-slab splitting measurements, as differences in plate motions among different reference frames are typically small (less than $\sim 30^{\circ}$).

The Central America subduction zone is characterized by subduction of the Cocos plate beneath the Caribbean plate in the south and the North American plate in the north. The dip of the subducting slab shallows northward along the trench with dips ranging from $\sim 16^{\circ}$ to $\sim 32^{\circ}$ [*Lallemand et al*., 2005]. Relative to the

© 2014. American Geophysical Union. All Rights Reserved.

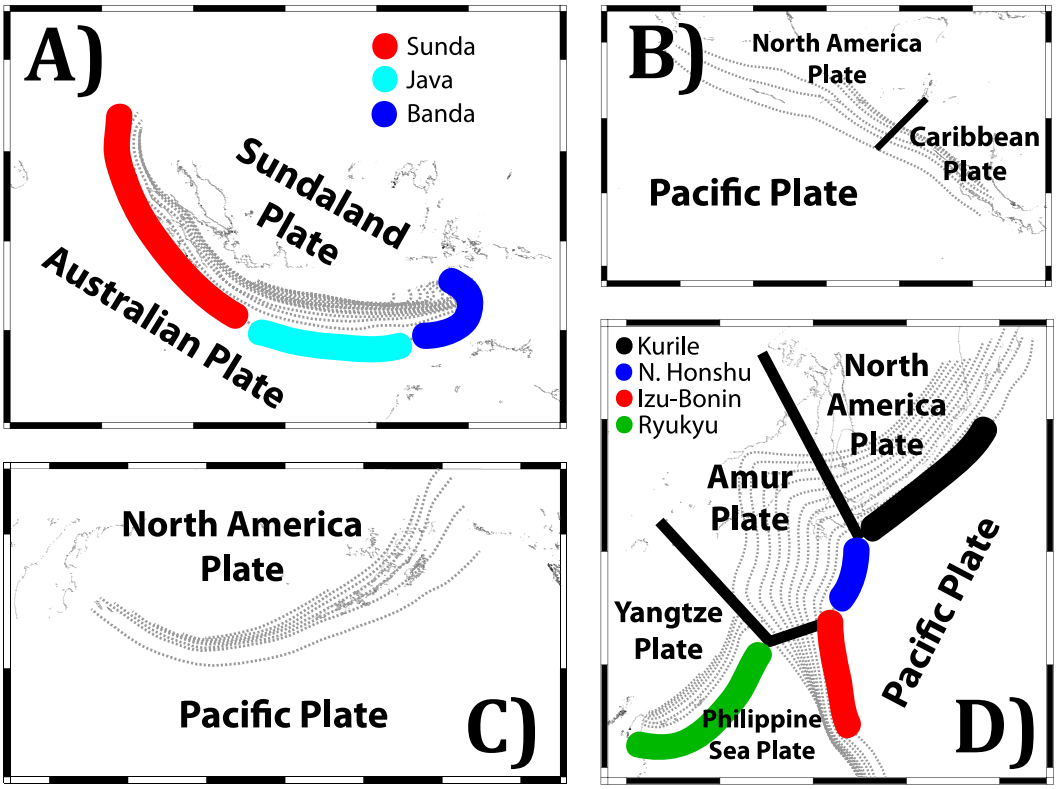

Figure 1. (a–d) Schematic diagrams of the tectonic plates and arc configurations in the Sumatra, Central America, Alaska-Aleutians, and Japan regions. The Kurile (black), Northern Honshu/Japan (blue), Izu-Bonin (red), and Ryukyu (green) trenches are highlighted in the (Figure 1d) Japan region, while the Sunda (red), Java-Andaman (light blue), and Banda (dark blue) arcs are highlighted in the (Figure 1a) Sumatra region.

Caribbean and North American plates, the Pacific plate is moving at a rate of ~8 cm/yr nearly perpendicular to the trench. The age of the downgoing plate varies from ~8 Ma in the north to ~27 Ma toward the south [*Heuret and Lallemand*, 2005].

The Alaska-Aleutians subduction zone is marked by subduction of the Pacific plate beneath the North American plate. The dip of the plate steepens toward the west from ~19° beneath Alaska to ~40° in the westernmost portion of the Aleutians [*Lallemand et al*., 2005]. The Pacific plate is moving at ~6.5 cm/yr relative to the North American plate. Due to the curvature of the trench, the motion of the Pacific plate relative to the overriding plate varies from nearly trench perpendicular beneath Alaska to roughly trench parallel in the westernmost part of the subduction zone where the plate boundary is roughly parallel to motion of the Pacific plate. The age of the subducting lithosphere increases westward from ~45 Ma in the east beneath Alaska to ~80 Ma in the west [*Heuret and Lallemand*, 2005].

The Japan-Ryukyu system is composed of the Kurile, Northern Honshu, Izu-Bonin, and Ryukyu subduction zones (Figure 1). The Kurile, Northern Honshu, and Izu-Bonin arcs are characterized by the subduction of the Pacific plate beneath the North American, Amur, and Philippine Sea plates, respectively. The Ryukyu subduction zone consists of the Philippine Sea plate subducting beneath the Yangtze plate. The motion of the Pacific plate relative to the North American, Amur, and Philippine Sea plates varies from trench oblique to trench perpendicular and are traveling at speeds of ~8.5, ~9.5, and ~4 cm/yr, respectively. The motion of the Philippine Sea plate relative to the Yangtze plate is predominantly trench normal with a velocity of ~8 cm/yr. The dip of the subducting plate beneath Kurile is ~36°. Beneath Northern Honshu, the dip is ~25°, and beneath Izu-Bonin, the dip is ~35°. The dip beneath Ryukyu is ~37° [*Lallemand et al*., 2005]. The age of the subducting Pacific lithosphere increases southward from Kurile where the subducting lithosphere is ~85 Ma to Izu-Bonin where the age is ~142 Ma. Beneath Ryukyu, the age of the subducting Philippine Sea plate ranges from ~25 to 47 Ma [*Heuret and Lallemand*, 2005]. Finally, the Sumatra subduction

© 2014. American Geophysical Union. All Rights Reserved.

system, here referring to the subduction beneath the Sunda, Java-Andaman, and Banda arcs, is characterized by subduction of the Australian plate beneath the Sundaland plate. East of ~120°E in this region, the slab begins to subduct continental lithospheric material [*Fichtner et al*., 2010]. Due to the curvature of the trench, the motion of the Australian plate relative to the Sundaland plate changes from trench normal in the south to nearly trench parallel in the northernmost portion of the region, leading to a situation where the motion of the downgoing plate is roughly parallel to the trench (similar to the western Aleutians). The velocity of the subducting plate varies from ~5 to ~7 cm/yr. The dip of the subducting slab varies from ~30° in the westernmost region to ~51° in the north [*Lallemand et al*., 2005]. The Sumatra subduction region is an ideal place to examine the effect of the age of the subducting lithosphere on sub-slab shear wave splitting patterns, as the age varies from 47 to 140 Ma [*Heuret and Lallemand*, 2005].

An important aspect of subduction zone kinematics is trench migration, which may control several aspects of mantle dynamics in subduction systems, perhaps including seismic anisotropy beneath subducting slabs [e.g., *Long and Silver*, 2009]. However, a quantitative evaluation of trench migration velocities requires a choice of reference frame, and estimates of trench migration rates vary widely based on choice of reference frame and plate motion model [e.g., *Funiciello et al*., 2008]. Therefore, we have not carried out quantitative comparisons between splitting observations and trench migration velocities in this paper. However, it is important to keep in mind that trench migration may be an important factor in controlling the dynamics of the sub-slab mantle.

3. Methods and Data

The source-side shear wave splitting technique takes advantage of seismicity in the source region to sample the anisotropy in the upper mantle near the earthquake sources. This technique is primarily applied to subduction zones [e.g., *Müller et al*., 2008a; *Russo*, 2009; *Russo et al*., 2010; *Foley and Long*, 2011; *Di Leo et al*., 2012; *Lynner and Long*, 2013; *Eakin and Long*, 2013] due to their abundant seismicity, but has also been applied to spreading ridges [*Nowacki et al*., 2012]. Using this technique in subduction zones allows for better sampling of the sub-slab mantle, and it has become popular in recent years. In this study, we select teleseismic direct *S* waves recorded at stations located at epicentral distances of 40–80° from the source region for analysis. This distance range is chosen to maximize the station coverage of the various subduction regions while minimizing the difference in incidence angle between the SK(K)S phases used to constrain the anisotropy beneath the seismic stations (as discussed below) and the teleseismic direct *S* waves used in the source-side technique. These factors trade off, however; as epicentral distance decreases, the incidence angles of direct S phases increase and thus further diverge from the nearly vertically incident SK(K)S phases used to constrain receiver-side anisotropy. The direct S phases sample two regions of anisotropy, namely the upper mantle beneath the source (i.e., the sub-slab mantle) and the upper mantle beneath the receiver. As in most source-side splitting studies, we assume that the bulk of the lower mantle away from subducting slabs is isotropic (Figure 2) [e.g., *Meade et al*., 1995].

As in our previous work [*Lynner and Long*, 2013], we restrict our analysis to seismic stations that exhibit simple splitting patterns due to upper mantle anisotropy beneath the receiver. Specifically, we use only seismic stations whose SK(K)S splitting patterns are consistent with either a single, horizontal layer of upper mantle anisotropy or an apparently isotropic upper mantle (Figure 2). Improper characterization or removal of the receiver-side anisotropy is a potential source of error in the source-side splitting technique. Rather than using previously published single-station average splitting parameters to remove the receiver-side signal, we reexamined SK(K)S splitting at over 200 long-running broadband seismic stations in regions located favorably with respect to the subduction zones under study. Out of this group, we selected 57 stations to use in our analysis (Figure 3) that are characterized by good backazimuthal SK(K)S coverage and simple splitting patterns (Figure 2).

We compared the SK(K)S measurements made in this study to previously published measurements where available, as compiled by *Wüstefeld et al*. [2009]. For the most part, our measurements generally agree with previously published values, despite differences in preprocessing and measurement choices. In a few cases, however, our measurements disagree to some extent with previously published values (for example, station SNZO in New Zealand [*Marson-Pidgeon and Savage*, 2004], and several island stations in the Indian Ocean [*Behn et al*., 2004]). One possible explanation for such discrepancies is frequency dependence; if splitting

© 2014. American Geophysical Union. All Rights Reserved.

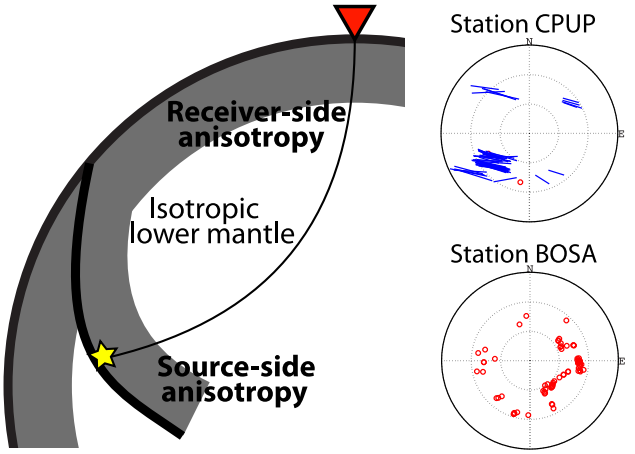

Figure 2. (left) Cartoon depicting the source-side splitting technique, which utilizes shear waves generated by slab earthquakes to sample the anisotropy in the mantle beneath subducting slabs. (right) Examples of simple splitting patterns recorded at stations used in this study. We show stereographic plots of null (circles) and nonnull (bars) SKS and SKKS splitting measurements recorded at stations CPUP in (bottom) South America and BOSA in (top) Africa. Splitting results are plotted as a function of backazimuth (angle from N) and incidence angle (distance from origin) with the orientation and length of the bars corresponding to fast splitting direction and delay time, respectively. Station BOSA (bottom) lies atop apparently isotropic upper mantle, as demonstrated by null splitting measurements over a range of backazimuths, while beneath station CPUP (top) we infer a single, flat-lying layer of anisotropy beneath the station, as demonstrated by consistent splitting at several different backazimuths.

beneath these stations depends on frequency and waveforms with different frequency contents were used, that could explain a difference in observed splitting. We have chosen to rely on our detailed, uniform SK(K)S measurements to constrain receiver-side anisotropy rather than on previous estimates, as splitting studies vary widely in methodology and frequency content and often lack sufficient backazimuthal coverage to reliably constrain splitting patterns. In any case, the use of a large number of stations in this study should minimize potential errors introduced by inaccurate receiver-side corrections at any given station.

For seismic stations that have been characterized as having simple splitting patterns, we remove the effect of anisotropy beneath the receiver from all incoming teleseismic *S* waves, following *Russo* [2009]. Specifically, we rotate the horizontal components to the observed receiver-side fast and slow directions and apply a time shift to the waveforms to remove the effect of splitting. Example waveforms that illustrate a typical receiver-side correction are shown in supporting information Figure S1. (A more detailed discussion of how receiver-side anisotropy is constrained in our study and how stations are

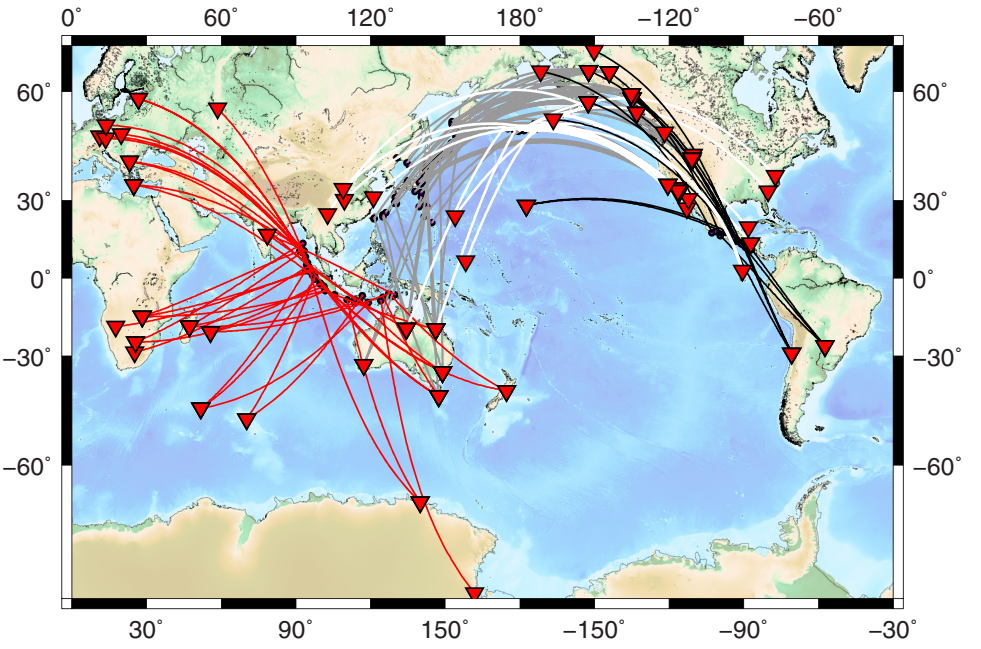

Figure 3. Map of all seismic stations used to make source-side splitting measurements in this study. Great circle paths connect seismic stations to subduction zones where those stations were used to constrain the sub-slab anisotropy. Black lines, white lines, gray lines, and red lines, respectively, connect stations to earthquake source regions beneath Central America, the Aleutians, the northwestern Pacific subduction zones, and Sumatra.

© 2014. American Geophysical Union. All Rights Reserved.

selected for analysis is contained in *Lynner and Long* [2013]; the removal of the receiver-side splitting signal is discussed in detail by *Russo* [2009].)

Our station distribution (Figure 3) ensures good coverage of the source regions studied here. Seismic stations in North America and South America were used to constrain sub-slab splitting in the Central America subduction zone. Stations in North America, Asia, Australia, and on various Pacific islands were used to examine sub-slab splitting for the Alaska-Aleutians subduction zone. Stations in Australia and North America recorded the sub-slab anisotropy in the Japan-Ryukyu system. Finally, stations in Africa, Europe, India, Antarctica, New Zealand, and on various Indian Ocean islands were used to measure sub-slab shear wave splitting in the Sumatra region. A table of all seismic stations examined in this study, whether they can or cannot be used for the source-side technique, and their associated receiver-side anisotropy corrections can be found in supporting information Table S1. Our approach allows us to accurately remove any splitting signal from anisotropy beneath the station and to minimize potential error due to inaccurate receiver-side corrections.

Events were selected by searching for slab earthquakes of magnitude Mw $>$ 5.0 in the Izu-Bonin, Ryukyu, Japan, Kurile, Alaska-Aleutians, Central America, and Sumatra subduction systems. Only events deeper than 20 km were considered in order to avoid sampling the crust on the source side. Although we carried out splitting measurements on all events deeper than 20 km and report results for earthquakes at all depths, only those shallower than 250 km are considered when interpreting splitting patterns of the upper mantle, as the deepest events may not necessarily reflect upper mantle anisotropy. They may instead be reflecting anisotropy in the transition zone or uppermost lower mantle [e.g., *Foley and Long*, 2011]. Our splitting measurements for deep ($>$250 km) events are reported and briefly discussed here, but their implications for mid-mantle anisotropy will be examined in more detail in a future paper.

Every seismogram was band-pass filtered to retain energy between periods of 8 and 25 s. This filter was chosen as it is suitable for retaining signal at the characteristic periods of both the direct *S* waves under study and the SK(K)S waves that were used to constrain receiver-side anisotropy, while removing microseismic noise at periods less than 8 s. We measured splitting of direct *S* waves using the Splitlab software package [*Wüstefeld et al*., 2008]. We visually inspected each waveform to ensure good signal-to-noise ratios. We identified misalignments of the horizontal components for several seismic stations used in this study (Table S1) based on systematic misfits between the incoming SKS polarization (particularly for null measurements) and the backazimuth. Several such stations have misalignment values recorded in their respective metadata, in good agreement with our misalignment observations derived from SK(K)S polarization analysis. Misalignment of the horizontal components can lead to systematic errors in splitting measurements [e.g., *Tian et al*., 2011; *Hanna and Long*, 2012; *Lynner and Long*, 2012]. We corrected for the observed misalignments of each station before any splitting measurements were carried out. These corrections can be found in supporting information Table S1.

As initial polarizations are not constrained by the source-receiver geometry for direct *S* waves, we used the eigenvalue minimization and rotation correlation methods simultaneously to determine the splitting parameters (fast direction, ϕ, and delay time, δt) for these phases. Neither method requires knowledge of the incoming polarization direction. The use of multiple splitting measurement methods simultaneously has been found to reproduce reliable results [e.g., *Wirth and Long*, 2010; *Huang et al*., 2011; *Eakin and Long*, 2013]. We only retained splitting measurements for which the two methods returned consistent results within their 2σ error spaces. Overall, simple nonweighted average errors in delay time are less than 0.4 s and average fast direction errors are less than 16° for the entire data set. The poorest measurements retained in our data set had 2σ rotation-correlation errors of less than $\pm$25° for ϕ and $\pm$ 0.9 s for δt. Null measurement characterizations were based on the linearity of uncorrected particle motion after correcting for receiver-side anisotropy. Measured source-side splitting parameters, along with their error estimates, can be found in supporting information Table S2.

4. Results

4.1. Regional Splitting Patterns

Nonnull shear wave splitting measurements attributed to the sub-slab mantle beneath the Japan-Ryukyu system, Alaska-Aleutians, Central America, and Sumatra regions are plotted in map view in Figures 4–7,

© 2014. American Geophysical Union. All Rights Reserved.

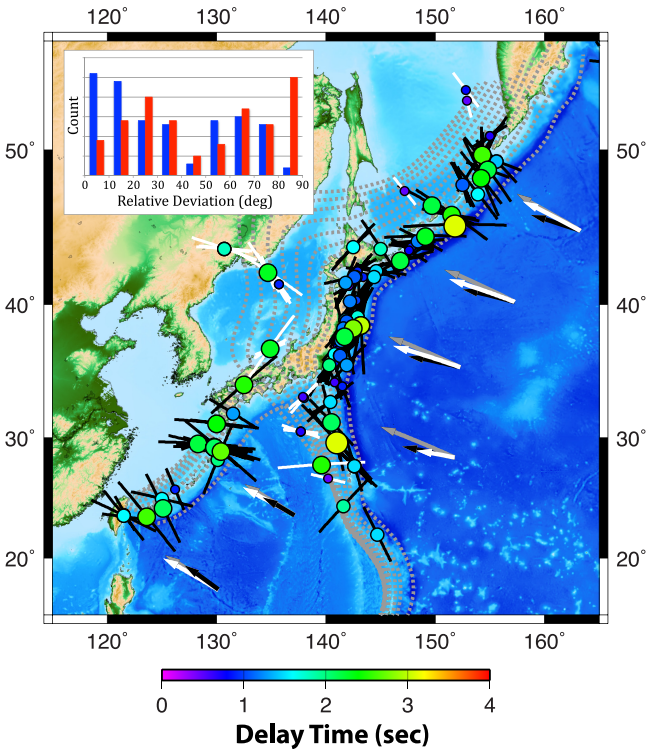

Figure 4. Source-side splitting results for the Japan-Ryukyu system. Sub-slab splitting parameters are plotted at the corresponding earthquake locations, with circles representing the earthquake epicenter. The color and size of the circles denote delay time. The orientation and length of the black (splitting from events shallower than 250 km) and white (splitting from events deeper than 250 km) bars correspond to the fast direction, ϕ, and delay time, δt. Measured fast directions were projected back along the raypath to reflect the geometry of anisotropy in the sub-slab mantle [e.g., *Foley and Long*, 2011]. Dashed gray lines show the slab contours of *Gudmundsson and Sambridge* [1998] at intervals of 50 km depth. The direction and length of the black and white arrows correspond to the motion (both direction and speed) of the subducting slab in the No-Net-Rotation (NNR) reference frame (black) and relative to upper plate (white) from the MORVEL plate motion model [*DeMets et al*., 2010]. The gray arrows correspond to the motion of the subducting plate in the hot spot reference frame (HS3-Nuvel-1A) from *Gripp and Gordon* [2002]. The inset histogram shows the deviation in measured fast directions from a trench parallel orientation (blue bars) and from a plate motion parallel orientation (red bars) for the entire region.

respectively. Maps of the distribution and orientation of null measurements can be found in supporting information Figures S2–S5. While we primarily compare our source-side shear wave splitting results to downgoing plate motions in the reference frame of the overriding plate using the MORVEL plate model [*DeMets et al*., 2010], we also plot downgoing plate motions for the No-Net-Rotation [*DeMets et al*., 2010] and the HS3-Nuvel-1A [*Gripp and Gordon*, 2002] reference frames (Figures 4–7). We will first discuss qualitatively the splitting patterns seen in each region, then discuss the entire data set as a whole and analyze the patterns more quantitatively (section 5).

The sub-slab anisotropy beneath Ryukyu (Figure 4) is illuminated by 25 nonnull and 10 null uppermost upper mantle source-side shear wave splitting measurements. The Ryukyu subduction zone is characterized by plate motion parallel fast splitting directions with an average delay time of 1.7 s. The Izu-Bonin subduction zone yielded the fewest source-side shear wave splitting measurements with 10 nonnull measurements. The fast directions exhibit trench parallel to trench oblique geometries, with an average delay time of 1.8 s. Beneath Japan (Honshu and Hokkaido), the abundant seismicity coupled with fortuitous event-station geometry allowed us to make 49 nonnull and 44 null uppermost mantle splitting measurements. Splitting in this region is very consistently trench parallel with an average delay time of 1.2 s. Our analysis of the Kurile subduction zone yielded 26 null and 41 nonnull splitting results, with a striking along-strike transition in fast splitting directions visible at ~46°N (despite some scatter in the data). Specifically, there is an abrupt change from roughly trench parallel fast splitting directions in southern Kurile to dominantly plate motion parallel splitting in the north. The average delay time in Kurile is 1.3 s (Figure 4).

Beneath the Alaska-Aleutians subduction zone, we measured 125 split and 45 unsplit shear waves. The fast direction varies along the strike of the trench, as does the trench strike itself, but a comparison between the fast directions and downgoing plate directions (Figure 5) reveals predominately plate motion parallel ϕ across the full extent of the trench. In the westernmost portion of the trench, the plate motion direction and the strike of the trench are nearly parallel; therefore, fast directions in that region are parallel to both plate motion and trench strike. In the center of the subduction zone, from roughly 175°E to −160°E, the fast directions have some scatter, but are roughly parallel to the motion of the Pacific plate relative to the North American plate. In the easternmost portion of the subduction zone, including subduction of the Pacific plate under continental North America beneath Alaska, fast directions are highly scattered, but a

© 2014. American Geophysical Union. All Rights Reserved.

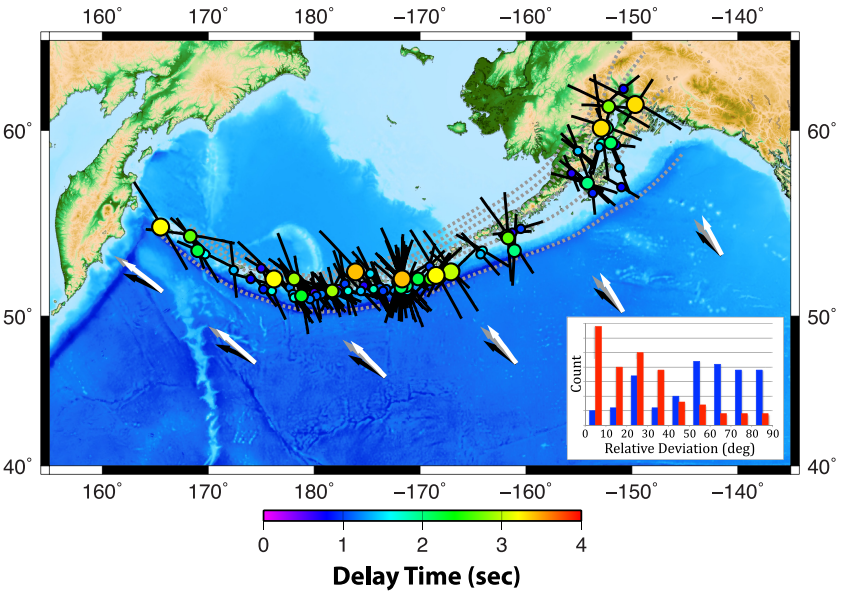

Figure 5. Source-side splitting results for the Alaska-Aleutians subduction zone. Plotting conventions are as in Figure 4. Note the scattered fast directions beneath Alaska and the dominantly plate motion parallel fast directions throughout the Aleutians; in the westernmost region, the motion of the Pacific plate is roughly parallel to the trench strike.

weak trend of fast directions that align roughly with the subducting plate motion may be present. The average delay time in the Alaska-Aleutians subduction zone is 1.6 s.

The Central America subduction zone (Figure 6) yielded 37 null and 78 nonnull measurements. The splitting pattern seen in Central America is consistent and quite simple. Plate motion parallel fast directions are seen along the entire length of the subduction zone, with an average delay time of 1.6 s. One interesting observation in this region is that the area with the highest amount of scatter, between −90°E and −95°E, corresponds to Motagua and Polochic fault zones [e.g., *Burkart*, 1978; *Franco et al*., 2009], which separate the North American and Caribbean plates.

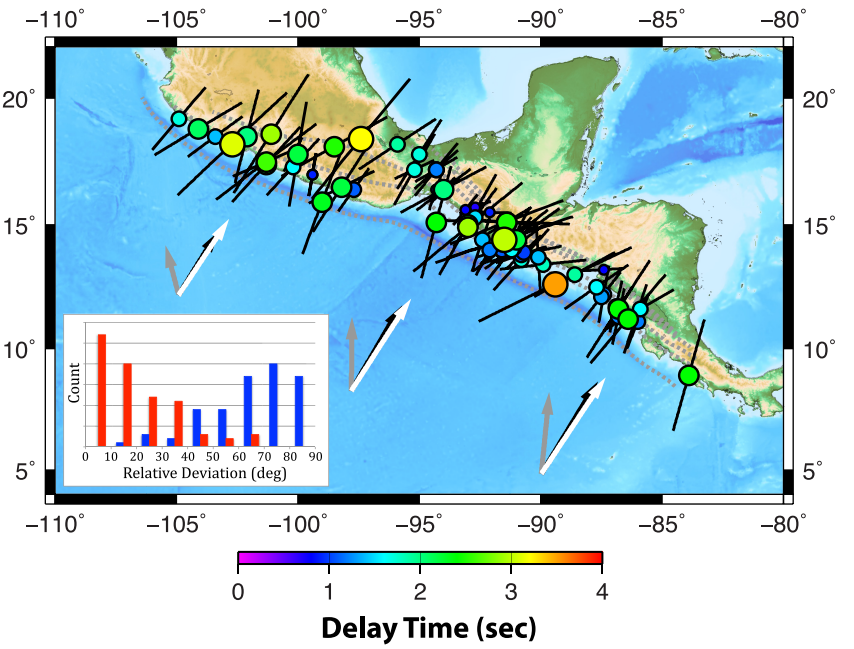

Figure 6. Source-side splitting results beneath Central America. Plotting conventions are as in Figure 4.

© 2014. American Geophysical Union. All Rights Reserved.

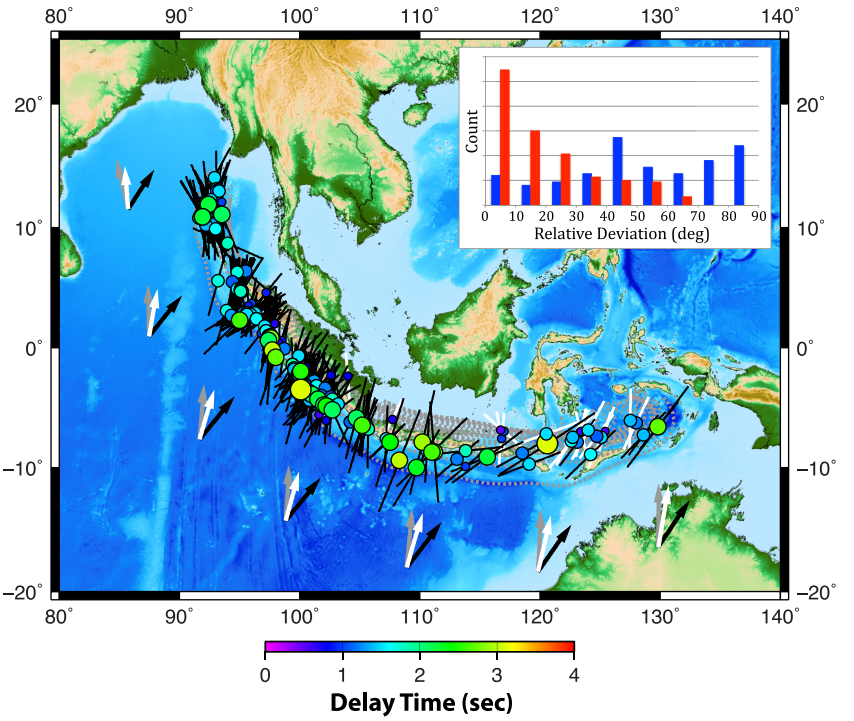

Figure 7. Source-side splitting results beneath Sumatra. Plotting conventions are as in Figure 4.

Finally, our source-side splitting data set for the Sumatra region comprises 202 splits and 96 nulls (Figure 7). The average delay time for splitting measurements in Sumatra is 1.4 s. The pattern in fast splitting directions seen beneath Sumatra is quite striking. Strong plate motion parallel splitting is seen throughout most of the subduction zone with two notable deviations, from 0°N to 5°N and east of ∼111°E. The northern deviation is small in extent and may correspond to a localized region of deformation associated with a diffuse boundary between the Australian and Indian plates [e.g., *DeMets et al*., 2010]. East of ∼111°E, we observe a striking change in fast splitting direction from plate motion parallel to roughly trench parallel orientations. This transition corresponds with the oldest part of the subducting lithosphere, and it is notable that a similar transition from plate motion parallel fast directions to trench parallel fast directions at a lithospheric age of ∼95 Ma is noted in the Kurile arc (in the Japan region). Importantly, this transition is located ∼1000 km west of the transition in type of subducting lithosphere (from oceanic to continental), so it does not appear to coincide with this change in the subduction properties. This transition in splitting direction we observe is consistent with SKS splitting seen in the region [*Hammond et al*., 2010].

To summarize, the splitting maps shown in Figures 4–7 demonstrate that while the various regions show differing degrees of scatter in the data, several broad trends are apparent. First, a striking aspect of this data set is the small variations in average delay times among different regions (from a maximum average delay time of 1.8 s in Izu-Bonin to a minimum of 1.2 s beneath Japan). Second, fast splitting directions that are parallel to the trench, generally thought to be the norm for the sub-slab region [e.g., *Long and Silver*, 2008, 2009], are not uniformly observed in our study. While there are several regions where trench parallel splitting is observed, such as beneath Northern Honshu, Izu-Bonin, the southernmost portion of the Kurile arc, and beneath eastern Indonesia in the Sumatra region, we have identified several regions that exhibit fast splitting directions roughly parallel to the motion of the downgoing plate, namely the Alaska-Aleutians, Central America, Ryukyu, the northern portion of Kurile, and western Sumatra subduction regions.

4.2. Observations of Splitting From Intermediate and Deep Earthquakes

Many of the regions examined (Izu-Bonin, Japan, Kurile, and Sumatra) exhibit measurable splitting for events deeper than 250 km (to depths greater than 600 km), shown in Figures 4 and 7. Beneath Japan, the deep splitting measurements exhibit roughly trench perpendicular fast directions, regardless of the observed splitting directions in the shallower mantle (Figure 4). Specifically, Honshu/Hokkaido and Izu-

© 2014. American Geophysical Union. All Rights Reserved.

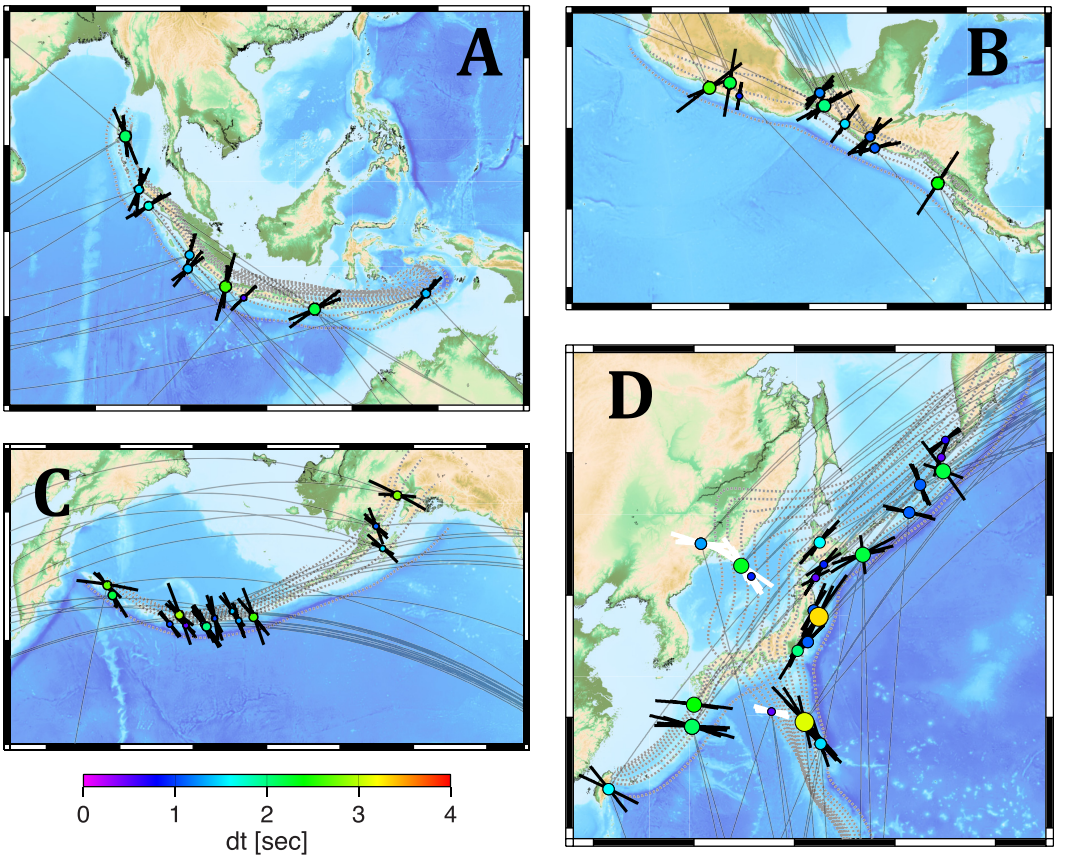

Figure 8. (a–d) Map views of the Sumatra region, Central America, the Alaska-Aleutians, and the Japan region showing a representative sample of measured splitting parameters for individual events that yielded measurements at several different stations. Thin black lines connect the events to the different stations at which splitting measurements were made.

Bonin are both characterized by trench parallel upper mantle sub-slab splitting, while northern Kurile is characterized by plate motion parallel splitting in the sub-slab mantle, yet all three areas exhibit trench perpendicular fast directions for the deep events. Beneath eastern Indonesia in the Sumatra region, however, the deep events exhibit a different pattern than beneath Japan, with roughly trench parallel to trench oblique fast directions for deep earthquakes (Figure 7), consistent with observations by *Di Leo et al*. [2012].

These observations of significant splitting from relatively deep events are striking and warrant further study. It is notable that some deep earthquakes in Japan and Sumatra regions yield delay times up to ~1.5 s, suggesting a contribution from anisotropy in the deep transition zone and/or uppermost lower mantle. These observations are consistent with recent observations of deep splitting beneath the Tonga subduction zone [*Chen and Brudzinski*, 2003; *Wookey and Kendall*, 2004; *Foley and Long*, 2011]; however, they are somewhat surprising, as the lower mantle is generally thought to be isotropic or nearly isotropic at such depths [*Meade et al*., 1995]. We are confident that our splitting measurements for deep events are robust, as they are individually well constrained, and we have identified several deep events that yield similar results at several different seismic stations (Figure 8). This observation precludes the possibility that the splitting signal is an artifact of improper receiver-side correction.

These deep splitting measurements represent unequivocal evidence for anisotropy at midmantle depths (transition zone and/or uppermost lower mantle). This observation complements recent similar observations of midmantle anisotropy [e.g., *Wookey et al*., 2002; *Foley and Long*, 2011; *Di Leo et al*., 2012; *Kaneshima*, 2014]. Interpretation of these measurements, however, remains difficult due to a paucity of information on the anisotropy and deformation of midmantle materials. Recently, *Kawazoe et al*. [2013] performed shear deformation experiments on wadsleyite (the dominant upper transition zone mineral) and found that the seismically anisotropic mineral can develop a preferred orientation resulting in polarization seismic

© 2014. American Geophysical Union. All Rights Reserved.

anisotropy. *Miyagi et al*. [2014], using high temperature and pressure experiments, successfully observed plastic anisotropy in ringwoodite (the dominant lower transition zone mineral). Using 3-D petrological-thermomechanical flow models and creep mechanisms simulations of crystal aggregates, *Faccenda* [2014] found that the midmantle may be weakly anisotropic with anisotropy concentrated around slabs. Additionally, *Faccenda* [2014] argues the uppermost lower mantle around slabs may be deforming via dislocation creep due to the high deviatoric stresses imposed by the slabs. This would result in LPO fabric development of perovskite, which is highly anisotropic [*Cordier et al*., 2004]. While wadsleyite is more strongly anisotropic than ringwoodite [e.g., *Mainprice*, 2007] and may therefore play a larger role in transition zone anisotropy, anisotropy due to wadsleyite cannot explain the deepest splitting measurements observed in this study, as we observe splitting from events originating beneath the upper transition zone. Anisotropy due to perovskite and/or ringwoodite must also be present to account for the observed deep splitting. Overall, the relationships between deformation and anisotropy for midmantle minerals remain poorly understood, and the interpretation of our deep splitting results in terms of mantle flow patterns remains challenging. We will address the geodynamical implications of these measurements, in combination with others from different regions, in a future paper.

5. Discussion

5.1. Fast Direction Patterns: General Characteristics

Our data set (Figures 4–7) demonstrates that most sub-slab fast splitting directions in the upper mantle are either nearly trench parallel or nearly plate motion parallel. There are many observations that do not fall exactly into these two categories, but these are the two dominant directions. Specifically, more than 70% of the measured fast directions fall within 25° of either the motion of the subducting plate or the strike of the trench. To test the statistical significance of this result, we constructed a simple test in which fast directions were generated randomly and compared to these two motions; this process was iterated 500 times to produce a vector of simulated estimates. We found that only 53.1% of these (purely randomly selected) fast directions fell within 25° of either motion. The 95% confidence intervals calculated around this mean value were 49.6% and 57.5%. The observed frequency of trench or plate motion parallel fast directions is therefore significantly different ($p = <0.05$) from the results of a null model simulating a large number of purely random directions, strongly suggesting that the measured fast directions have nonrandom orientations. The Central America, Ryukyu, much of the Alaska-Aleutians, the northern portion of the Kurile, and most of the Sumatra region are all characterized by source-side splitting that is dominantly parallel to the motion of the subducting plate. In contrast, the Japan, Izu-Bonin, the southern portion of the Kurile, and the eastern portion of the Sumatra region beneath Indonesia present trench parallel fast directions. Beneath the westernmost portions of both Sumatra and the Aleutians, the situation is ambiguous as the motion of the downgoing plate is nearly parallel to the local strike of the trench. The variability in fast directions that we observe in our data set suggests that a mix of processes may control sub-slab mantle anisotropy.

The most striking conclusion that emerges from our data set is that trench parallel sub-slab fast splitting directions may not be as common as previously thought. Previous global compilations of sub-slab shear wave splitting parameters [*Long and Silver*, 2008, 2009] suggested that trench parallel splitting was nearly ubiquitous beneath slabs, with only a few exceptions (e.g., Cascadia, Mexico, and the central part of South America). For the most part, these measurements were based on previously published estimates of teleseismic splitting corrected for the effect of wedge anisotropy. Since then, as the more accurate source-side splitting technique has been applied in new regions, previous estimates have been borne out in some regions (e.g., the Caribbean, Scotia, Tonga, Northern Honshu) [*Foley and Long*, 2011; *Lynner and Long*, 2013, and this study], but contradicted in others (Ryukyu, Central America, parts of Sumatra; this study). Additionally, since the compilation of *Long and Silver* [2009], several additional regions in which plate motion parallel sub-slab fast splitting directions appear to dominate have been identified (e.g., beneath the flat subduction segment in Peru [*Eakin and Long*, 2013]; beneath southern Chile [*Hicks et al*., 2012]; beneath Sumatra [*Collings et al*., 2013; *Hammond et al*., 2010]).

Source-side shear wave splitting studies offer good spatial coverage of the sub-slab mantle, which allows us to observe lateral variations in splitting along-strike beneath the various subduction zones. This is

© 2014. American Geophysical Union. All Rights Reserved.

important, as we observed lateral variations in splitting behavior within individual subduction zones in this study, with rapid lateral transitions between the two (over length scales of a few hundred kilometers or less).

5.2. Possible Sources of Error

A concern when interpreting source-side splitting data sets like those presented here is the potential contamination of the source-side signal from receiver-side anisotropy. Splitting of direct S phases may be due to anisotropy either beneath the source or beneath the seismic station, as discussed above, so it is crucial to ensure that the receiver-side splitting signal is properly removed. One way to test whether our receiver-side corrections (described in section 3) are effectively removing splitting due to anisotropy beneath the receiver is to examine splitting parameters obtained for a single event at multiple stations. If the receiver-side anisotropy is properly removed and the anisotropy in the source region is relatively simple (and thus the splitting parameters do not depend strongly on azimuth or takeoff angle), splitting measurements for a single event should be consistent across several stations. We examined events with multiple measurements in each subduction zone and found that this is generally true for our data set. Several examples for the various subduction zones are shown in Figure 8. These comparisons reveal that while there are slight variations in some of the measured splitting parameters for individual events, $\sim$74% of measured fast directions and $\sim$69% of measured delay times for events with multiple measurements fall within 20° and 0.8 s of each other, respectively (within typical measurement errors). These tests lend confidence to our measurements, and also help to demonstrate that in general, we do not observe significant variations in observed splitting as a function of event-to-station azimuth, which suggests relatively simple anisotropic structure beneath many slabs.

A possible source of ambiguity in the interpretations of our measurements comes from the potential influence of the slab itself on the measured splitting. Oceanic lithosphere develops frozen-in anisotropy as it matures [e.g., *Montagner and Tanimoto*, 1991; *Maggi et al*., 2006; *Debayle and Ricard*, 2013]. It has been shown that plates retain this frozen-in anisotropy through subduction [e.g., *Huang et al*., 2011; *Baccheschi et al*., 2011; *Song and Kim*, 2012; *Audet*, 2013; *Eakin and Long*, 2013]. Estimates of slab anisotropy vary greatly depending on region and method used. *Song and Kim* [2012] estimate $\sim$7% anisotropy in the uppermost portion of the subducting Cocos slab using receiver functions. *Huang et al*. [2011] and *Baccheschi et al*. [2011] estimate the contribution to observed shear wave splitting from subducting plates in Japan and in Italy to be minor ($\sim$0.1 s), while *Eakin and Long* [2013] suggest that anisotropy in the subducting slab beneath Peru may be strong. It appears that anisotropy in subducting slabs is present albeit in potentially different amounts depending on the region. As such, it is possible that source-side splitting measurements reflect anisotropy both in the subducting slab and anisotropy in the sub-slab mantle.

This issue may be particularly acute for the northern part of Central America and the eastern Alaska-Aleutians, given the geographical limitations in station selection for these regions (Figure 3). In general, we strove to minimize slab contamination by choosing seismic stations that lie in an updip direction relative to the subduction geometry (such that direct S rays take off in a direction opposite to the dip of the slab) thus minimizing the volume of slab sampled. However, the location of the Pacific Ocean relative to northern Central America and the eastern Alaska-Aleutians limits the station availability, so we included stations with event-to-station azimuths that were close to the strike of the trench. For these stations, the S rays may travel within the slab for a significant distance. For these two regions, we explored the potential effect of slab anisotropy on our measurements by comparing measurements for favorable and less-favorable raypath geometries. For northern Central America, the effect of slab anisotropy seems to be negligible, as there are several events that yielded similar splitting measurements at stations that sample minimal amounts of slab anisotropy and those with longer slab raypaths. For example, splitting at stations CPUP and DOT for a single Central American event yielded very similar results (fast directions $62° < 78° < 92°$ and $53° < 72° < 92°$ and delay times of 1.4 s $<$ 1.7 s $<$ 2.0 s and 0.5 s $<$ 1.1 s $<$ 1.8 s, respectively) despite very different event-station paths. The path to DOT samples up to 250 km of slab while the slab portion of the path to CPUP is much smaller (less than $\sim$100 km).

Most of the raypaths included in our study for the eastern Aleutians (beneath Alaska) also likely travel significant distances through the subducting slab. Unlike in the Central America subduction zone, signal contamination from the slab seems to be present. Potential slab contamination may explain the large amounts of scatter in the source-side splitting data set beneath this region (Figure 5). We chose to include these

© 2014. American Geophysical Union. All Rights Reserved.

measurements here for the sake of completeness, but the splitting in the eastern Aleutians should be interpreted with caution. For the rest of regions explored in this study, the event-station geometries are such that there should be minimal sampling of the subducting slabs.

5.3. Comparison With Previous Studies

For the vast majority of previous studies, sub-slab anisotropy was inferred by first determining splitting due to mantle wedge anisotropy using local-S phases, then removing that wedge splitting signal from the observed SK(K)S (or teleseismic direct S) measurements. (We refer to this as the "teleseismic S minus local S method" in the ensuing discussion; see *Long and Silver* [2009] for a more detailed description of how sub-slab anisotropy is inferred using teleseismic S and local S phases.) Using this method, weak trench parallel sub-slab splitting was inferred beneath the Aleutians and beneath Ryukyu [*Long and Silver*, 2008], trench parallel to trench oblique splitting was inferred beneath Northern Honshu [*Nakajima and Hasegawa*, 2004]. Strong trench parallel splitting was inferred beneath Central America by *Abt et al*. [2010], and beneath Kamchatka (to the north of our measurements for the Kurile arc), trench parallel fast directions were inferred [*Peyton et al*., 2001; *Levin et al*., 2004; *Long and Silver*, 2008]. In the Sumatra region, sub-slab fast directions have been interpreted to be trench parallel beneath eastern Indonesia and roughly plate motion parallel throughout the rest of the Sumatra region [*Hammond et al*., 2010], similar to what is seen in this study. Using the source-side method, *Di Leo et al*. [2012] measured roughly trench parallel splitting beneath eastern Indonesia, and *Russo and Silver* [1994] observed primarily trench oblique splitting beneath Central America. In many regions, our inferences of sub-slab anisotropy based on source-side splitting measurements are consistent with previous estimates based on SK(K)S splitting measurements. However, we observed pronounced discrepancies between the measurement methods between the Aleutians, Ryukyu, and Central America subduction zones.

Previous estimates of sub-slab anisotropy based on SK(K)S and local S phases vary widely in the (qualitative) error estimates for sub-slab shear wave splitting parameters, for a variety of reasons. In many regions (like the Aleutians), poor station coverage, poor event coverage, and/or poorly constrained wedge anisotropy imply that the sub-slab anisotropy signal cannot be tightly constrained using SK(K)S and local S. In particular, the mantle wedge often exhibits very complicated anisotropy patterns [e.g., *Long and Wirth*, 2013, and references therein] and a precise correction for the effect of wedge anisotropy on SK(K)S splitting is often difficult. For this reason, it is difficult to assess the accuracy of these sub-slab anisotropy inferences, which is why the use of the source-side splitting technique in these regions offers particular value.

Beneath Central America and Ryukyu, however, previous studies have taken advantage of relatively good station coverage and relatively abundant slab seismicity; in both regions, both teleseismic and local shear wave splitting have been investigated in detail, as discussed below. It is therefore interesting that the sub-slab anisotropy geometry inferred from source-side shear wave splitting beneath these two specific regions and the geometry inferred from previous studies of these regions are quite different. We identified plate motion parallel fast splitting directions beneath both regions using the source-side method, yet previous estimates based on teleseismic and local S inferred trench parallel sub-slab splitting using the teleseismic S minus local S method described above. In order to investigate the source(s) of these discrepancies, we have carried out a careful comparison between the direct S raypaths used in this study and the raypaths used by previous studies to probe both wedge and sub-slab anisotropy.

Upper mantle anisotropy beneath Central America has been extensively studied by *Abt et al*. [2009, 2010]. In particular, the study of *Abt et al*. [2010] compared the strong SK(K)S splitting observed beneath stations of the TUCAN experiment, with trench parallel fast directions and large ($\sim$2 s) delay times, to the much weaker splitting measured for the mantle wedge region [*Hoernle et al*., 2008; *Abt et al*., 2009], and inferred strong trench parallel splitting beneath the Central America slab. A unique aspect of the *Abt et al*. [2010] study is that the authors explicitly corrected the individual SK(K)S waveforms for the effect of the wedge, using a detailed 3-D model for wedge anisotropy [*Abt et al*., 2009] obtained from shear wave splitting tomography [*Abt and Fischer*, 2008]. The careful approach taken by *Abt et al*. [2010] to account for the effect of wedge anisotropy means that the discrepancy between their observations and ours is particularly puzzling. A potential contribution to this discrepancy is the possibility of frequency-dependent splitting, which has been documented in several subduction zone settings [e.g., *Marson-Pidgeon and Savage*, 1997; *Eakin and Long*, 2013]. However, we do not view this as the likely primary explanation for the strong discrepancy

© 2014. American Geophysical Union. All Rights Reserved.

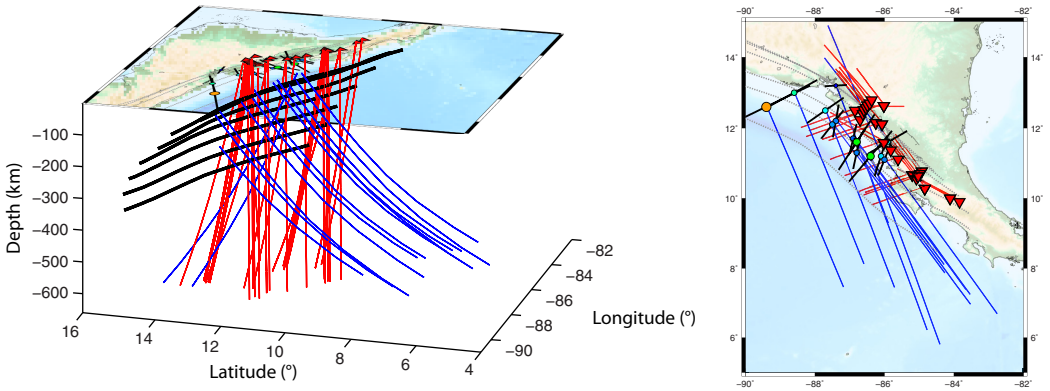

Figure 9. (right) Map view and (left) oblique three-dimensional view of the rays used in our Central America source-side study (blue) and the SK(K)S rays used in the *Abt et al*. [2010] sub-slab anisotropy study (red). The two different types of phases used have little to no overlap in the upper mantle, effectively sampling different volumes of the sub-slab mantle. In map view (right), it can be seen that the source-side rays take off toward the southeast, while the SK(K)S rays arrive from the northwest and southwest.

between the SK(K)S results and our measurements, as the SK(K)S splitting patterns documented by *Abt et al*. [2010] are dramatically different than those documented here (that is, ∼2 s of trench parallel splitting versus ∼1 s of trench perpendicular splitting). It is difficult to attribute this dramatic difference solely to complex and frequency-dependent anisotropy in the mantle wedge.

To further investigate this issue, we produced a three-dimensional plot of the SK(K)S raypaths used by *Abt et al*. [2010] and the direct S phases used in our study, shown in Figure 9. This plot demonstrates that the two different types of phases study sample quite different volumes of the sub-slab mantle. Directly beneath the slab, they sample similar material, but they quickly diverge from each other in the deeper parts of the upper mantle (Figure 9). The discrepancy in the observed splitting, therefore, is most likely due to this difference in sampling. This raises the intriguing possibility that there may be multiple layers of sub-slab anisotropy beneath Central America. One potential explanation for the discrepancy is that there is a region of dominantly trench parallel anisotropy in the deep upper mantle or transition zone, while the shallower upper mantle corresponds to plate motion parallel anisotropy. This pattern is similar to predictions from recent numerical modeling by *Di Leo et al*. [2014], which took strain history into account when predicting anisotropy. The discrepancy in inferred sub-slab splitting patterns beneath Central America between different measurement methods implies some complexity in sub-slab anisotropic structure.

We carried out a similar comparison for the Ryukyu region between our raypaths and those used in previous studies [*Long and van der Hilst*, 2005, 2006; *Long and Silver*, 2008]. Weak trench parallel splitting with very small delay times was inferred by *Long and Silver* [2008] from the data sets of *Long and van der Hilst* [2005, 2006] using teleseismic S phases while accounting for anisotropy in the mantle wedge. Ryukyu suffers from very poor backazimuthal coverage for SK(K)S phases, so in order to increase backazimuthal coverage, *Long and van der Hilst* [2005] used direct teleseismic *S* waves from deep events in Tonga and in Sumatra in addition to SK(K)S. In order to mitigate any potential source-side anisotropic signal contribution in the teleseismic *S* waves, *Long and van der Hilst* [2005] used only deep events (>300 km) and performed several tests to minimize any contribution to the observed splitting from anisotropy near the source.

Interestingly, a plot of the raypaths used in *Long and van der Hilst* [2005] and in this study (Figure 10) reveals that they sample the sub-slab mantle in nearly identical ways. Therefore, the discrepancy in sub-slab splitting between our study and that inferred by *Long and Silver* [2008] based on the measurements of *Long and van der Hilst* [2005, 2006] cannot be due to differential sampling of the sub-slab mantle, as in Central America. Instead, we propose that the most likely cause of this discrepancy is an oversimplified characterization of mantle wedge anisotropy in the calculations of *Long and Silver* [2008]. A complete characterization of mantle wedge anisotropy is difficult in any subduction zone, as wedge anisotropy is often very complicated [*Long and Wirth*, 2013, and references therein] and the spatial distribution of stations on the overriding plate is often limited. Therefore, oversimplified models for wedge anisotropy may increase the errors associated with estimates of sub-slab splitting obtained by correcting teleseismic phases for the effect of

© 2014. American Geophysical Union. All Rights Reserved.

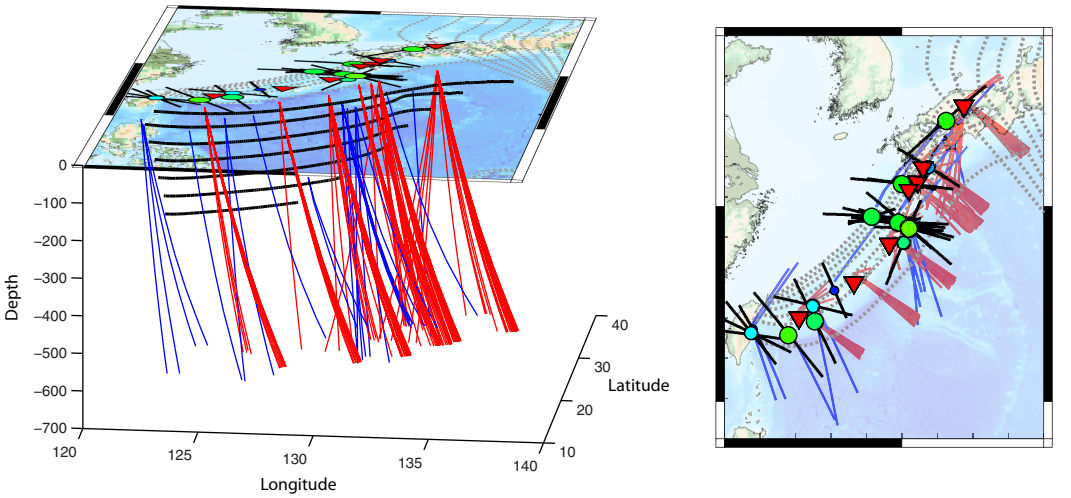

Figure 10. (right) Map view and (left) oblique three-dimensional of the rays used in our Ryukyu source-side study (blue) and the SK(K)S and direct teleseismic S rays used in the *Long and van der Hilst* [2005] upper mantle anisotropy study (red). Both views demonstrate that the source-side rays (blue) and the rays from the *Long and van der Hilst* [2005] study (red) overlap substantially in the sub-slab mantle. The only substantial difference is the sampling of the mantle wedge by all of the *Long and van der Hilst* [2005] rays (red).

the wedge. Detailed forward modeling of Ryukyu wedge anisotropy has been carried out [*Kneller et al*., 2008] and geodynamic models for wedge flow that incorporate B-type olivine fabric have been found to match the local S splitting observations of *Long and van der Hilst* [2006] well. However, subsequent studies that have used anisotropic receiver functions to examine the wedge beneath Ryukyu have identified extremely complex structure, with as many as four different anisotropic layers oriented in different directions [*McCormack et al*., 2013]. This level of complexity would not have been apparent in the local-S shear wave splitting previously used to constrain wedge anisotropy [*Long and van der Hilst*, 2006]. We suggest, therefore, that the most likely explanation for the discrepancy between the two methods is that the anisotropic structure of the mantle wedge beneath Ryukyu is more complicated than that reflected in the estimates of *Long and Silver* [2008] for anisotropy beneath the slab.

Another potential explanation for the discrepancy is possible contamination of the Ryukyu upper mantle anisotropy estimates by anisotropy in the source region of the direct teleseismic *S* waves used in the study of *Long and van der Hilst* [2005]. There is observational evidence for splitting due to source-side anisotropy beneath Tonga [*Wookey and Kendall*, 2004 for receivers located in Australia; *Foley and Long*, 2011 for receivers located in North America] and beneath Sumatra [*Di Leo et al*., 2012 for receivers in Asia and India; this study, using receivers located in Africa, Europe, India, Antarctica, New Zealand, and on various Indian Ocean islands], which suggests the possibility of some source-side contamination of the *Long and van der Hilst* [2005] data set. However, as previously argued by *Long and van der Hilst* [2005], a pervasive contribution from anisotropy near the earthquake sources is unlikely for at least three reasons. First, if source-side contamination were a primary contributor to the teleseismic S data set, we would not expect significant variations in splitting parameters among nearby stations in Japan, but such variations were observed. Second, strong contributions from source-side anisotropy would imply significant and systematic differences in splitting among different source regions, which is not consistent with the *Long and van der Hilst* [2005] observations. Third, SK(K)S phases measured at Ryukyu stations were found to have generally similar splitting as the teleseismic direct S phases. Therefore, while some source-side contamination in the *Long and van der Hilst* [2005] data set remains a possibility, the most likely explanation for the discrepancy in inferred sub-slab splitting behavior is an incomplete characterization of mantle wedge anisotropy in the estimates by *Long and Silver* [2008].

5.4. Relationship Between Splitting Patterns and Subducting Plate Age

Why do some regions exhibit trench parallel splitting while others are dominated by plate motion parallel splitting? For most parameters that describe subduction (e.g., slab dip, convergence velocity, takeoff angle, slab width, ray azimuth, etc.), we did not identify any noticeable correlations between sub-slab splitting behavior and other subduction zone parameters (supporting information Figure S6). We also considered

© 2014. American Geophysical Union. All Rights Reserved.

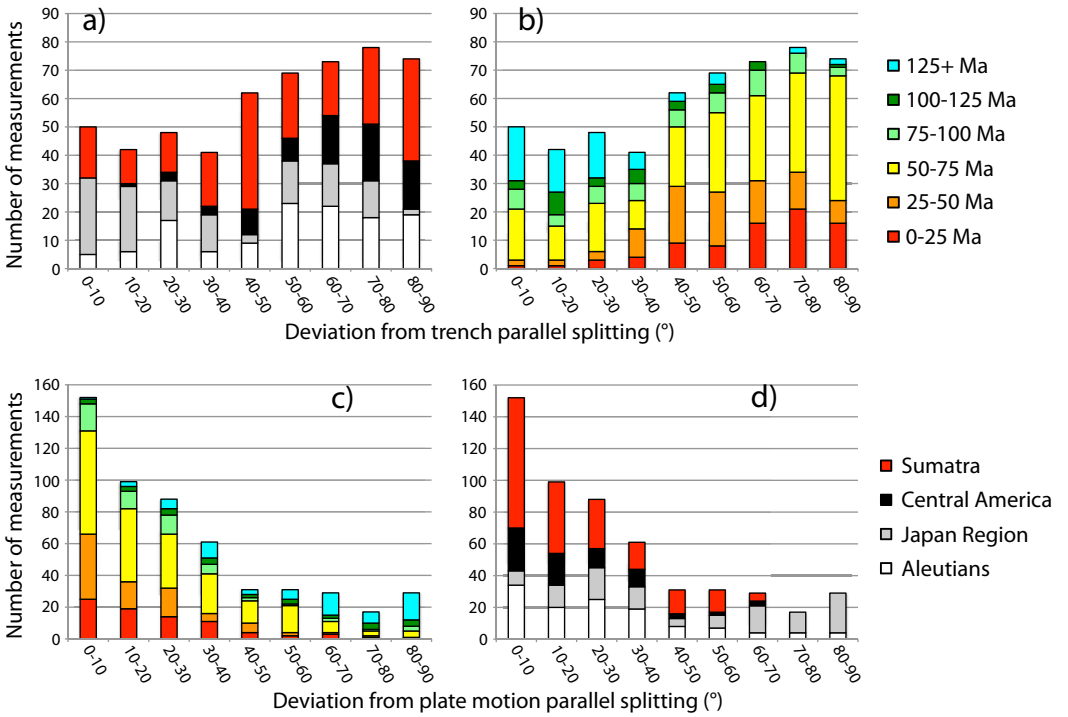

Figure 11. Histogram plots of observed sub-slab splitting directions. We plot (a and b) the deviation of the measured fast directions from the local strike of the trench and (c and d) the deviation of the measured fast directions from the local direction of the downgoing plate. Figures 11a and 11d color-coded by region, while Figures 11b and 11c are color-coded by the age of the subducting lithosphere (legends are on the right).

the possibility of a change in olivine LPO fabric, either laterally or with depth, from one in which fast splitting directions tend to align with the direction of maximum finite strain (A, C, or E types) to one in which fast directions align orthogonally to maximum strain (B type). We consider this to be an unlikely explanation, as the upper mantle beneath subducting slabs is likely to be relatively warm and dry; B-type fabric requires high stresses, low temperatures, and the presence of water [*Karato et al*., 2008]. A possible pressure-induced fabric transition to B-type fabric has also been suggested [*Jung et al*., 2009] at a depth of ~90 km, but there is no evidence from either the data set presented here or our previous source-side splitting studies [*Foley and Long*, 2012; *Lynner and Long*, 2013] for a change in splitting behavior at this depth.

There is a striking correlation between sub-slab splitting behavior and the age of the subducting lithosphere, as shown in Figures 11 and 12. Plate age may therefore represent a controlling parameter for sub-slab anisotropy. Specifically, the transition from plate motion parallel to trench parallel splitting seems to correlate well with the age of the subducting lithosphere, with older lithosphere generally exhibiting trench parallel splitting and younger lithosphere exhibiting plate motion parallel splitting. This pattern is apparent from both a comparison among different subduction zones and within individual subduction systems, such as Sumatra and Kurile. For both Sumatra and Kurile, there is a clear and rapid change in the pattern of sub-slab shear wave splitting that occurs at a lithospheric age of approximately 95 Ma. This relationship is easily seen in Figure 11, where we plot histograms of the angular deviation between fast splitting directions and both trench strike and plate motion directions as histograms. Immediately apparent is the lack of young lithospheric ages and the abundance of old ages in cases in which the fast directions are trench parallel, while the opposite is true for cases in which splitting directions are parallel to the motion of the subducting slab.

Based on the data presented in this study, we hypothesize that sub-slab shear wave splitting behavior is controlled by the age of the subducting lithosphere, with a relatively sharp transition from plate motion parallel to trench parallel fast directions occurring at a lithospheric age of ~95 Ma. Such a conceptual model does an excellent job of predicting the sub-slab observations presented here, as shown in Figure 12. In a companion paper (Lynner and Long, 2014), we tested this hypothesis quantitatively by combining the data

© 2014. American Geophysical Union. All Rights Reserved.

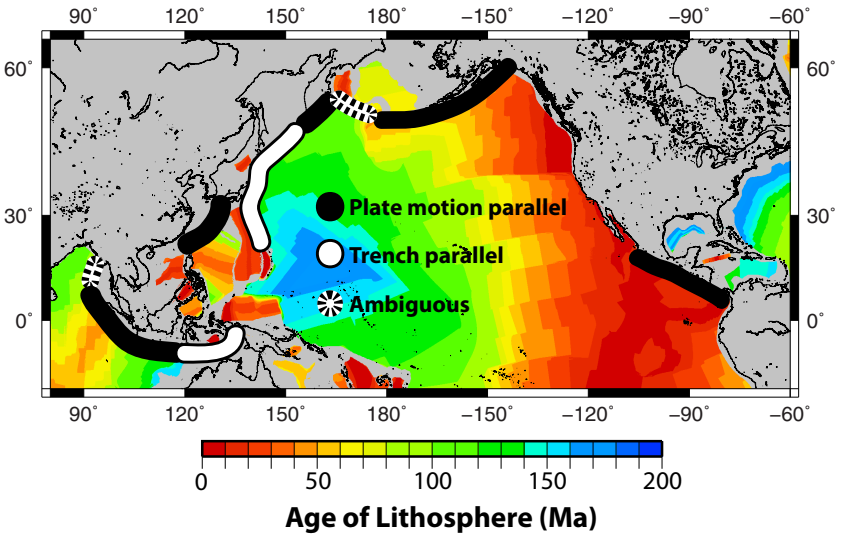

Figure 12. Map view schematic of the general patterns in sub-slab fast splitting directions identified in this study. Background colors indicate the age of the oceanic lithosphere from *Müller et al*. [2008b]. Old ages of subducting lithosphere generally correspond to trench parallel splitting, while young lithosphere generally correlates with plate motion parallel splitting.

sets presented here with other previously published studies that used identical processing techniques [*Foley and Long*, 2011; *Lynner and Long*, 2013] to obtain a quasi-global source-side splitting data set. We used these measurements to quantitatively test how well the conceptual model of lithospheric age-dependent splitting explains the global observations, as well as other models of sub-slab anisotropy (the 3-D return flow model of *Long and Silver* [2008, 2009] and the entrained asthenosphere model of *Song and Kawakatsu* [2012, 2013]). We found that a model in which splitting is controlled by the age of the downgoing slab matches the global observations better than either a simplified 3-D return flow model [*Long and Silver*, 2008, 2009] or the entrained asthenosphere model [*Song and Kawakatsu*, 2012, 2013].

The geodynamic implications of our age-dependent model are discussed in detail in Lynner and Long (2014), but we briefly discuss some aspects here. Several characteristics of subduction systems depend on the age of the subducting lithosphere, including the slab thickness, the possible onset of small-scale convection beneath the oceanic lithosphere, and possibly the characteristics of the oceanic lithosphere-asthenosphere boundary. Because slab thickness is a thermally controlled parameter that changes gradually with age, it is an unlikely explanation for the sharp transition in dominant fast direction with age documented in this study. We propose, instead, that there is a relatively rapid change in the nature of the mechanical coupling beneath subducting slabs at a slab age of ~95 Ma. A transition from strong coupling beneath younger lithosphere to decoupling beneath older lithosphere would allow for the sub-slab mantle to transition from a 2-D entrained flow regime beneath younger slabs to a 3-D return flow regime, induced by trench migration, beneath older slabs. Such a transition in the sub-slab flow field would be consistent with the change in fast directions orientations documented in this study. One possible mechanism for a change in sub-slab coupling is the onset of small-scale convection beneath older lithosphere.

6. Summary

Previous estimates of anisotropy in the sub-slab mantle have mainly relied on a combination of teleseismic shear waves (usually SK(K)S) and local *S* waves that constrain and account for anisotropy in the complex region of the mantle wedge [e.g., *Long and Silver*, 2008, 2009]. In this study, we have implemented a more direct and accurate method for estimating anisotropy beneath subducting slabs, using the source-side splitting technique with accurate receiver-side corrections. We have presented source-side splitting measurements for the Alaska-Aleutians, Izu-Bonin-Japan-Kurile, Ryukyu, Sumatra, and Central America subduction systems. We observe two first-order classes of fast splitting directions beneath the various regions. Japan, Izu-Bonin, southern Kurile, and eastern Sumatra all exhibit roughly trench parallel splitting directions, while northern Kurile, much of the Alaska-Aleutians, Central America, and western Sumatra are dominated by

© 2014. American Geophysical Union. All Rights Reserved.

plate motion parallel splitting. Observed delay times in the different subduction zones are quite uniform with average delay times ranging from 1.3 to 1.8 s. Beneath Japan, Kurile, Izu-Bonin, and Sumatra, we also observe splitting from deep (deeper than 250 km) sources, indicating a contribution from anisotropy at transition zone or midmantle depths near the subducting slabs.

The observed dichotomy in fast splitting direction (predominantly trench parallel or plate motion parallel) is an interesting observation, as previous studies had inferred trench parallel sub-slab splitting in many subduction zones globally [e.g., *Long and Silver*, 2008, 2009]. Our observation of both plate motion parallel and trench parallel splitting directions beneath different regions and within individual regions indicates complexity in the sub-slab flow field. Interestingly, the dichotomy in splitting directions correlates well with the age of the subducting lithosphere. Trench parallel sub-slab splitting appears to correlate with the subduction of older oceanic lithosphere (older than ~95 Ma), while plate motion parallel fast directions are seen where younger lithosphere is subducting (younger than ~95 Ma). One possible mechanism for this age-dependent pattern is small-scale convection (or other factors) acting to decouple the slab from the sub-slab mantle beneath older regions, resulting in entrained two-dimensional sub-slab flow beneath young slabs and three-dimensional flow induced by trench migration beneath old slabs.

Acknowledgments

Data used in this study came from a variety of seismic networks, including the Global Seismograph Network (II, IU), Global Telemetered Seismic Network (GT), United States National Seismic Network (US), Caltech Regional Seismic Network (CI), Alaska Regional Network (AK), Alaska Tsunami Warning Seismic System (AT), New China Digital Seismograph Network (IC), Czech Regional Seismic Network (CZ), Caribbean Network (CU), ANZA Regional Network (AZ), NARS Array (NR), Polish Seismological Network (PL), German Regional Seismic Network (GR), Geoscope (G), Geofon (GE), Pacific21 (PS), Intermountain West (IW), and Mednet (MN) networks. All data were accessed via the Data Management Center (DMC) of the Incorporated Research Institutions for Seismology (IRIS). Many figures were prepared using the Generic Mapping Tools [*Wessel and Smith*, 1991]. This work was funded by NSF grant EAR-1150722. We are grateful to David Bercovici, Jeffrey Park, David Evans, and Shun Karato for useful discussions on sub-slab anisotropy. Finally, we thank Martha Savage and two anonymous reviewers for helpful comments that greatly improved this paper.

References

Abt, D. L., and K. M. Fischer (2008), Resolving three-dimensional anisotropic structure with shear-wave splitting tomography, *Geophys. J. Int.*, *173*, 859–889.

Abt, D. L., K. M. Fischer, G. A. Abers, W. Strauch, J. M. Protti, and V. González (2009), Shear wave anisotropy beneath Nicaragua and Costa Rica: Implications for flow in the mantle wedge, *Geochem. Geophys. Geosyst.*, *10*, Q05S15, doi:10.1029/2009GC002375.

Abt, D. L., K. M. Fischer, G. A. Abers, M. Protti, V. González, and W. Strauch (2010), Constraints on upper mantle anisotropy surrounding the Cocos slab from SK(K)S splitting, *J. Geophys. Res.*, *115*, B06316, doi:10.1029/2009JB006710.

Audet, P. (2013), Seismic anisotropy of subducting oceanic uppermost mantle from fossil spreading, *Geophys. Res. Lett.*, *40*, 173–177, doi:10.1029/2012GL054328.

Baccheschi, P., L. Margheriti, M. S. Steckler, and E. Boschi (2011), Anisotropy patterns in the subducting lithosphere and in the mantle wedge: A case study—The southern Italy subduction system, *J. Geophys. Res.*, *116*, B08306, doi:10.1029/2010JB007961.

Behn, M. A., C. P. Conrad, and P. Silver (2004), Detection of upper mantle flow associated with the African superplume, *Earth Planet. Sci. Lett.*, *224*, 259–274.

Billen, M. I. (2008), Modeling the dynamics of subducting slabs, *Annu. Rev. Earth Planet. Sci.*, *36*, 325–356.

Burkart, B. (1978), Offset across the Polochic fault of Guatemala and Chiapas, *Mexico, Geology*, *6*(6), 328–332.

Chen, W.-P., and M. R. Brudzinski (2003), Seismic anisotropy in the mantle transition zone beneath Fiji-Tonga, *Geophys. Res. Lett.*, *30*(13), 1682, doi:10.1029/2002GL016330.

Collings, R., A. Rietbrock, D. Lange, F. Tilmann, S. Nippress, and D. Natawidjaja (2013), Seismic anisotropy in the Sumatra subduction zone, *J. Geophys. Res.*, *118*, 5372–5390, doi:10.1002/jgrb.50157.

Cordier, P., T. Ungár, L. Zsoldos, and G. Tichy (2004), Dislocation creep in $MgSiO_3$ perovskite at conditions of the Earth's uppermost lower mantle, *Nature*, *428*(6985), 837–840.

Debayle, E., and Y. Ricard (2013), Seismic observations of large-scale deformation at the bottom of fast-moving plates, *Earth Planet. Sci. Lett.*, *376*, 165–177, doi:10.1016/j.epsl.2013.06.025.

DeMets, C., R. G. Gordon, and D. F. Argus (2010), Geologically current plate motions, *Geophys. J. Int.*, *181*, 1–80, doi:10.1111/j.1365-246X.2009.04491.x.

Di Leo, J., A. Walker, Z.-H. Li, J. Wookey, N. Ribe, J.-M. Kendall, and A. Tommasi (2014), Development of texture and seismic anisotropy during the onset of subduction, *Geochem. Geophys. Geosyst.*, *15*, 192–212, doi:10.1002/2013GC005032.

Di Leo, J. F., J. Wookey, J. O. S. Hammond, J.-M. Kendall, S. Kaneshima, H. Inoue, T. Yamashina, and P. Harjadi (2012), Mantle flow in regions of complex tectonics: Insights from Indonesia, *Geochem. Geophys. Geosyst.*, *13*, Q12008, doi:10.1029/2012GC004417.

Eakin, C. M., and M. D. Long (2013), Complex anisotropy beneath the Peruvian flat slab from frequency-dependent, multiple-phase shear wave splitting analysis, *J. Geophys. Res.*, *118*, 4794–4813, doi:10.1002/jgrb50349.

Faccenda, M. (2014), Mid mantle seismic anisotropy around subduction zones, *Phys. Earth Planet. Inter.*, *227*, 1–19, doi:10.1016/j.pepi.2013.11.015.

Faccenda, M., and F. A. Capitanio (2013), Seismic anisotropy around subduction zones: Insights from three-dimensional modeling of upper mantle deformation and SKS splitting calculations, *Geochem. Geophys. Geosyst.*, *14*, 243–262, doi:10.1029/2012GC004451.

Faccenda, M., L. Burlini, T. V. Gerya, and D. Mainprice (2008), Fault-induced seismic anisotropy by hydration in subducting oceanic plates, *Nature*, *455*, 1097–1110.

Fichtner, A., M. de Wit, and M. van Bergen (2010), Subduction of continental lithosphere in the Banda Sea region: Combining evidence from full waveform tomography and isotope ratios, *Earth Planet. Sci. Lett.*, *297*, 405–412, doi:10.1093/gji/ggs131.

Foley, B. J., and M. D. Long (2011), Upper and mid-mantle anisotropy beneath the Tonga slab, *Geophys. Res. Lett.*, *38*, L02303, doi:10.1029/2010GL046021.

Franco, A., E. Molina, H. Lyon-Caen, J. Vergne, T. Monfret, A. Nercessian, S. Cortez, O. Flores, D. Monterosso, and J. Requenna (2009), Seismicity and crustal structure of the Polochic-Motagua fault system area (Guatemala), *Seismol. Res. Lett.*, *80*, 977–984.

Funiciello, F., C. Faccenna, A. Heuret, S. Lallemand, E. Di Giuseppe, and T. W. Becker (2008), Trench migration, net rotation and slab–mantle coupling, *Earth Planet. Sci. Lett.*, *271*(1–4), 233–240, doi:10.1016/j.epsl.2008.04.006.

Gripp, A. E., and R. G. Gordon (2002), Young tracks of hotspots and current plate velocities, *Geophys. J. Int.*, *150*, 321–361.

Gudmundsson, O., and M. Sambridge (1998), A regionalized upper mantle (RUM) seismic model, *J. Geophys. Res.*, *103*, 7121–7136, doi:10.1029/97JB02488.

Hammond, J. O. S., J. Wookey, S. Kaneshima, H. Inoue, T. Yamashina, and P. Harjadi (2010), Systematic variation in anisotropy beneath the mantle wedge in the Java-Sumatra subduction system from shear wave splitting, *Phys. Earth Planet. Inter.*, *178*, 189–201.

© 2014. American Geophysical Union. All Rights Reserved.

Hanna, J., and M. D. Long (2012), SKS splitting beneath Alaska: Regional variability and implications for subduction processes at a slab edge, *Tectonophysics*, *530–531*, 272–285.
Heuret, A., and S. Lallemand (2005), Plate motions, slab dynamics and back-arc deformation, *Phys. Earth Planet. Inter.*, *149*, 31–51, doi: 10.1016/j.pepi.2004.08.022.
Hicks, S. P., S. E. J. Nippress, and A. Rietbrock (2012), Sub-slab mantle anisotropy beneath south-central Chile, *Earth Planet. Sci. Lett.*, *357*, 203–213.
Hoernle, K., D. L. Abt, K. M. Fischer, H. Nichols, F. Hauff, G. Abers, P. van den Bogaard, G. Alvarado, M. Protti, and W. Strauch (2008), Geochemical and geophysical evidence for arc-parallel flow in the mantle wedge beneath Costa Rica and Nicaragua, *Nature*, *451*, 1094–1098, doi:10.1038/nature06550.
Huang, Z., D. Zhao, and L. Wang (2011), Shear wave anisotropy in the crust, mantle wedge, and subducting Pacific slab under northeast Japan, *Geochem. Geophys. Geosyst.*, *12*, Q01002, doi:10.1029/2010GC003343.
Jung, H., W. Mo, and H. W. Green (2009), Upper mantle seismic anisotropy resulting from pressure-induced slip transition in olivine, *Nat. Geosci.*, *2*, 73–77.
Kaneshima, S. (2014), Upper bounds of seismic anisotropy in the Tonga slab near deep earthquake foci and in the lower mantle, *Geophys. J. Int.*, *197*, 351–368, doi:10.1093/gji/ggt494.
Karato, S., H. Jung, I. Katayama, and P. Skemer (2008), Geodynamic significance of seismic anisotropy of the upper mantle: New insights from laboratory studies, *Annu. Rev. Earth Planet Sci.*, *36*, 59–95.
Kawazoe, T., T. Ohuchi, Y. Nishihara, N. Nishiyama, K. Fujino, and T. Irifune (2013), Seismic anisotropy in the mantle transition zone induced by shear deformation of wadsleyite, *Phys. Earth Planet. Inter.*, *216*, 91–98.
King, S. D. (2007), Mantle downwellings and the fate of subducting slabs: Constraints from seismology, geoid topography, geochemistry, and petrology, *Treatise Geophys.*, *7*, 325–370.
Kneller, E. A., M. D. Long, and P. E. van Keken (2008), Olivine fabric transitions and shear-wave anisotropy in the Ryukyu subduction system, *Earth Planet. Sci. Lett.*, *268*, 268–282.
Lallemand, S., A. Heuret, and D. Boutelier (2005), On the relationships between slab dip, back-arc stress, upper plate absolute motion, and crustal nature in subduction zones, *Geochem. Geophys. Geosyst.*, *6*, Q09006, doi:10.1029/2005GC000917.
Levin, V., D. Droznin, J. Park, and E. Gordeev (2004), Detailed mapping of seismic anisotropy with local shear waves in southeastern Kamchatka, *Geophys. J. Int.*, *158*, 1009–1023, doi:10.1111/j.1365-246X.2004.02352.x.
Long, M. D. (2013), Constraints on subduction geodynamics from seismic anisotropy, *Rev. Geophys.*, *51*, 76–112, doi:10.1002/rog.20008.
Long, M. D., and T. W. Becker (2010), Mantle dynamics and seismic anisotropy, *Earth Planet. Sci. Lett.*, *297*, 341–354.
Long, M. D., and P. G. Silver (2008), The subduction zone flow field from seismic anisotropy: A global view, *Science*, *319*, 315–318.
Long, M. D., and P. G. Silver (2009), Mantle flow in subduction systems: The sub-slab flow field and implications for mantle dynamics, *J. Geophys. Res.*, *114*, B10312, doi:10.1029/2008JB006200.
Long, M. D., and R. D. van der Hilst (2005), Upper mantle anisotropy beneath Japan from shear wave splitting, *Phys. Earth Planet. Inter.*, *151*, 206–222.
Long, M. D., and R. D. van der Hilst (2006), Shear wave splitting from local events beneath the Ryukyu arc: Trench-parallel anisotropy in the mantle wedge, *Phys. Earth Planet. Inter.*, *155*, 300–312.
Long, M. D., and E. A. Wirth (2013), Mantle flow in subduction systems: The wedge flow field and implications for wedge processes, *J. Geophys. Res.*, *118*, 583–606, doi:10.1002/jgrb.50063.
Lynner, C., and M. D. Long (2012), Evaluating contributions to SKKS splitting from lower mantle anisotropy: A case study from station DBIC, Côte D'Ivoire, *Bull. Seismol. Soc. Am.*, *102*, 1030–1040.
Lynner, C., and M. D. Long (2013), Sub-slab seismic anisotropy and mantle flow beneath the Caribbean and Scotia subduction zones: Effects of slab morphology and kinematics, *Earth Planet. Sci. Lett.*, *361*, 367–378.
Maggi, A., E. Debayle, K. Priestley, and G. Barruol (2006), Azimuthal anisotropy of the Pacific region, *Earth Planet. Sci. Lett.*, *250*, 53–71.
Mainprice, D. (2007), Seismic anisotropy of the deep Earth from a mineral and rock physics perspective, *Treatise. Geophys.*, *2*, 437–491.
Marson-Pidgeon, K., and M. K. Savage (1997), Frequency-dependent anisotropy in Wellington, New Zealand, *Geophys. Res. Lett.*, *24*, 3297–3300.
Marson-Pidgeon, K., and M. K. Savage (2004), Modelling shear wave splitting observations from Wellington, New Zealand, *Geophys. J. Int.*, *157*(2), 853–864.
McCormack, K., E. A. Wirth, and M. D. Long (2013), B-type olivine fabric and mantle wedge serpentinization beneath the Ryukyu arc, *Geophys. Res. Lett.*, *40*, 1697–1702, doi:10.1002/grl.50369.
Meade, C., P. G. Silver, and S. Kaneshima (1995), Laboratory and seismological observations of lower mantle isotropy, *Geophys. Res. Lett.*, *22*, 1293–1296.
Miyagi, L., G. Amulele, K. Otsuka, Z. Du, R. Farla, and S. I. Karato (2014), Plastic anisotropy and slip systems in ringwoodite deformed to high shear strain in the Rotational Drickamer Apparatus, *Phys. Earth Planet. Inter.*, *228*, 244–253, doi:10.1016/j.pepi.2013.09.012.
Montagner, J.-P., and T. Tanimoto (1991), Global upper mantle tomography of seismic wave velocities and anisotropies, *J. Geophys. Res.*, *96*, 20,337–20,351.
Müller, C., B. Bayer, A. Eckstaller, and H. Miller (2008a), Mantle flow in the South Sandwich subduction environment from source-side shear wave splitting, *Geophys. Res. Lett.*, *35*, L03301, doi:10.1029/2007GL032411.
Müller, R. D., M. Sdrolias, C. Gaina, and W. R. Roest (2008b), Age spreading rates and spreading asymmetry of the world's ocean crust, *Geochem. Geophys. Geosyst.*, *9*, Q04006, doi:10.1029/2007GC001743.
Nakajima, J., and A. Hasegawa (2004), Shear-wave polarization anisotropy and subduction-induced flow in the mantle wedge of northern Japan, *Earth Planet. Sci. Lett.*, *225*, 365–377.
Nowacki, A., J.-M. Kendall, and J. Wookey (2012), Mantle anisotropy beneath the Earth's mid-ocean ridges, *Earth Planet. Sci. Lett.*, *317–318*, 56–67.
Peyton, V., V. Levin, J. Park, M. Brandon, J. Lees, E. Gordeev, and A. Ozerov (2001), Mantle flow at a slab edge: Seismic anisotropy in the Kamchatka region, *Geophys. Res. Lett.*, *28*, 379–382.
Russo, R. M. (2009), Subducted oceanic asthenosphere and upper mantle flow beneath the Juan de Fuca slab, *Lithosphere*, *1*, 195–205.
Russo, R. M., and P. G. Silver (1994), Trench-parallel flow beneath the Nazca Plate from seismic anisotropy, *Science*, *263*, 1105–1111.
Russo, R. M., A. Gallego, D. Comte, V. I. Moncau, R. E. Murdie, and J. C. VanDecar (2010), Source-side shear wave splitting and upper mantle flow in the Chile Ridge subduction zone, *Geology*, *38*, 707–710.
Savage, M. K. (1999), Seismic anisotropy and mantle deformation: What have we learned from shear wave splitting, *Rev. Geophys.*, *37*, 65–106.

© 2014. American Geophysical Union. All Rights Reserved.

Schellart, W. P. (2007), The potential influence of subduction zone polarity on overriding plate deformation, trench migration and slab dip angle, *Tectonophysics*, *445*, 363–372.
Silver, P. G. (1996), Seismic anisotropy beneath the continents: Probing the depths of geology, *Annu. Rev. Earth Planet. Sci.*, *24*, 385–432.
Silver, P. G., and W. W. Chan (1991), Shear wave splitting and subcontinental mantle deformation, *J. Geophys. Res.*, *96*, 16,429–16,454.
Song, T.-R. A., and H. Kawakatsu (2012), Subduction of oceanic asthenosphere: Evidence from sub-slab seismic anisotropy, *Geophys. Res. Lett.*, *39*, L17301, doi:10.1029/2012GL052639.
Song, T.-R. A., and H. Kawakatsu (2013), Subduction of oceanic asthenosphere: A critical appraisal in central Alaska, *Earth Planet. Sci. Lett.*, *367*, 82–94.
Song, T.-R. A., and Y. Kim (2012), Anisotropic upper mantle in young subducted slab underplating Central Mexico, *Nat. Geosci.*, *5*, 55–59.
Tian, X., J. Zhang, S. Si, J. Wang, Y. Chen, and Z. Zhang (2011), SKS splitting measurements with horizontal component misalignment, *Geophys. J. Int.*, *185*, 329–340.
van Keken, P. E. (2003), Structure and dynamics of the mantle wedge, *Earth Planet. Sci. Lett.*, *215*, 323–338.
Vinnik, L. P., and R. Kind (1993), Ellipticity of teleseismic S-particle motion, *Geophys. J. Int.*, *113*(1), 165–174.
Wessel, P., and W. H. F. Smith (1991), Free software helps map and display data, *Eos Trans. AGU*, *72*, 441.
Wirth, E., and M. D. Long (2010), Frequency-dependent shear wave splitting beneath the Japan and Izu-Bonin subduction zones, *Phys. Earth Planet. Inter.*, *181*, 141–154.
Wookey, J., and J.-M. Kendall (2004), Evidence of midmantle anisotropy from shear wave splitting and the influence of shear-coupled P waves, *J. Geophys. Res.*, *109*, B07309, doi:10.1029/2003JB002871.
Wookey, J., J.-M. Kendall, and G. Barruol (2002), Mid-mantle deformation inferred from seismic anisotropy, *Nature*, *415*, 777–780.
Wüstefeld, A., G. Bokelmann, G. Barruol, and C. Zaroli (2008), Splitlab: A shear-wave splitting environment in Matlab, *Comput. Geosci.*, *34*, 515–528.
Wüstefeld, A., G. Bokelmann, G. Barruol, and J. P. Montagner (2009), Identifying global seismic anisotropy patterns by correlating shear-wave splitting and surface-wave data, *Phys. Earth Planet. Inter.*, *176*(3), 198–212.
Zhao, D. (2001), Seismological structure of subduction zones and its implications for arc magmatism and dynamics, *Phys. Earth Planet. Inter.*, *127*, 197–214.

© 2014. American Geophysical Union. All Rights Reserved.